Journal of Power Sources 185 (2008) 207–211

Contents lists available at ScienceDirect

Journal of Power Sources

journal homepage: www.elsevier.com/locate/jpowsour

Short communication

Performance of strontium- and magnesium-doped lanthanum gallate electrolyte with lanthanum-doped ceria as a buffer layer for IT-SOFCs

Dokyol Lee [a], Ju-Hyeong Han [a,*], Eun-Gu Kim [a], Rak-Hyun Song [b], Dong-Ryul Shin [b]

[a] Department of Materials Science and Engineering, Korea University, 5-1 Anam-dong, Seongbuk-gu, Seoul 136-713, Republic of Korea
[b] Hydrogen & Fuel Cell Research Department, Korea Institute of Energy Research, 71-2 Jang-dong, Yuseong-gu, Daejeon 305-600, Republic of Korea

ARTICLE INFO

Article history:
Received 14 March 2008
Received in revised form 15 May 2008
Accepted 2 June 2008
Available online 20 June 2008

Keywords:
Solid oxide fuel cell
Electrolyte
Buffer layer
Cell test
Lanthanum-doped ceria
Power density

ABSTRACT

$La_{0.8}Sr_{0.2}Ga_{0.8}Mg_{0.2}O_{2.8}$ (LSGM8080) powder, showing the highest electrical conductivity among LSGMs of various compositions, is synthesized using the glycine nitrate process (GNP) and used as the electrolyte for an intermediate-temperature solid oxide fuel cell (IT-SOFC). The LDC ($Ce_{0.55}La_{0.45}O_{1.775}$) powder is synthesized by a solid-state reaction and employed as the material for a buffer layer to prevent the reaction between the anode and electrolyte materials. The LDC also serves as the skeleton material for the anode. An anode-supported single cell with an active area of 1 cm^2 is constructed for performance evaluation. A single-cell test is performed at 750 and 800 °C. The maximum power density of the cell 459 and 664 mW cm^{-2} at 750 and 800 °C, respectively.

1. Introduction

$La_{1-x}Sr_xGa_{1-y}Mg_yO_{3-\delta}$ (LSGM) is one of the materials that many fuel cell developers are considering as a potential candidate to replace the state-of-the-art yttria-stabilized zirconia (YSZ) electrolyte for intermediate-temperature solid oxide fuel cells (IT-SOFCs), mainly due to its high oxygen-ion conductivity. In addition, LSGM has attracted particular attention because it shows mechanical stability and long-term durability [1–4]. Nevertheless, the chemical instability of LSGM has so far prevented its use as an electrolyte for IT-SOFCs. It has been reported [5] that the reaction occurring at the Ni-based anode|LSGM electrolyte interface during sintering leads to degradation of cell performance, due to the formation of insulating reaction products. The occurrence of the interface reaction has been confirmed in our laboratory [6].

According to the data of Huang et al. [4], who systematically synthesized LSGMs via a solid-state reaction while varying both *x* and *y* over the compositional range from 0.05 to 0.3 in steps of 0.05, $La_{0.80}Sr_{0.20}Ga_{0.83}Mg_{0.17}O_{3-\delta}$ (LSGM8083: a combination of La and Ga atomic percentages is used in this symbolic system) showed the highest conductivity at 800 °C. On the other hand, LSGM8080 gave the highest conductivity in our previous data [6]. In that study, however, it has to be noted that the conductivity measurements were made for only four compositions, namely: LSGM9090, LSGM9080, LSGM8090 and LSGM8080

In this investigation, an attempt is made to use a chemically-stable LDC (45 mol% lanthanum-doped ceria) buffer layer to prevent the reaction between Ni and LSGM at the anode|electrolyte interface. The LDC is prepared via a solid-state reaction and also used as the anode skeleton material. The composition of LSGM is chosen as the one with the highest conductivity. For this purpose, LSGMs with the compositions, 8080 and 8083, which were previously reported to exhibit the highest conductivity, are prepared by the glycine nitrate process (GNP) and their conductivities are measured for comparison. A single-cell test is conducted at intermediate-temperatures of 750 and 800 °C with and without the buffer layer to examine its effect.

2. Experimental procedure

2.1. Sample preparation

LSGM powders with the compositions 8080 and 8083 were synthesized by means of the GNP and calcined at 1000 °C for 2 h. Commercial powders of $La(NO_3)_3{\cdot}6H_2O$, $Sr(NO_3)_2$, $Ga(NO_3)_3{\cdot}xH_2O$

* Corresponding author. Tel.: +82 2 32903813; fax: +82 2 9283584.
E-mail addresses: dylee@korea.ac.kr (D. Lee), hanjuh99@korea.ac.kr (J.-H. Han), keg0710@nate.com (E.-G. Kim), rhsong@kier.re.kr (R.-H. Song), drshin@korea.ac.kr (D.-R. Shin).

0378-7753/$ – see front matter © 2008 Elsevier B.V. All rights reserved.
doi:10.1016/j.jpowsour.2008.06.028

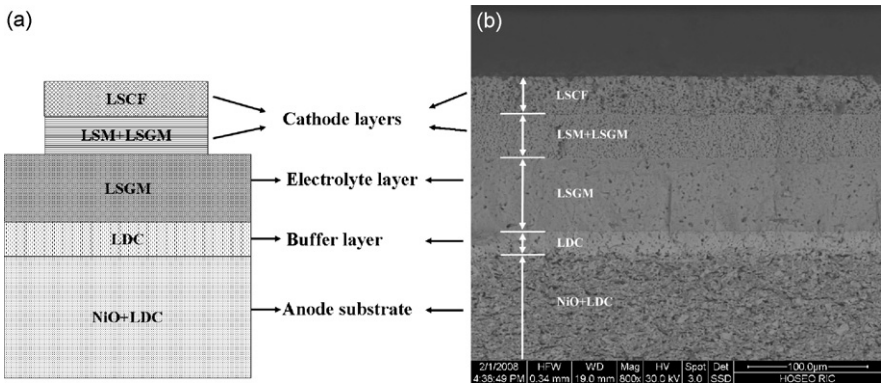

Fig. 1. (a) Schematic configuration and (b) cross-sectional BSE micrograph of anode-supported single-cell.

and $Mg(NO_3)_2{\cdot}6H_2O$ (Kojundo Chemical) were used as the starting materials together with glycine (Duksan Chemical). The details of the synthesis procedure have been described in earlier work [6]. The synthesized powder was compacted into a disc (20 mm Ø) and sintered at 1400 °C for 4 h in air for characterization. The LDC powder was prepared from La_2O_3 and CeO_2 powders (Kanto Chemical) by the solid-state reaction at 1400 °C for 3 h. Prior to the reaction, a mixture of the two powders with an La:Ce molar ratio of 45:55 were ball milled in ethyl alcohol for 48 h and the slurry was dried in an oven.

The phases of the sintered LSGM and of the synthesized LDC were identified by means of X-ray diffraction analysis (XRD, Rigaku Geigerflex, DMAX-IIA). The microstructures of the sintered LSGM were observed through a field emission scanning electron microscope (FE-SEM, Hitachi S-4300). The electrical conductivities of the LSGM were measured at various temperatures between 500 and 800 °C using ac two-probe impedance analysis (Hewlett-Packard, HP4192A) and the composition with the maximum conductivity was determined from the gathered data. Platinum paste was painted on both sides of a disc specimen and fired at 900 °C for 3 h to form the electrodes necessary for the measurement. Once the composition of maximum conductivity was determined, only the LSGM ,with that composition, was used in the subsequent experiments and the other compositions were no longer considered.

2.2. Chemical stability of LDC buffer layer

In order to examine the chemical stability of the LDC layer in contact with LSGM, a powder mixture of LDC and LSGM with a weight ratio of 1:1 was prepared. For uniform mixing, the mixture was wet-milled in a mortar using an agent of ethyl alcohol. After drying, it was heated at 1400 °C for 4 h (this was actually the sintering condition for the specimen with successive layers of LDC and LSGM on top of the anode-support) to ensure a sufficient reaction between the two materials. Finally, the material was crushed into a powder again in a mortar for XRD analysis, in order to examine whether or not there were any reaction products formed during heating.

2.3. Single-cell tests

For single-cell tests, an anode-supported cell with an active area of 1 cm^2 was constructed, as shown in the schematic diagram presented in Fig. 1(a). A powder mixture of 45 vol.%NiO/LDC together with activated carbon as a pore former was ball milled in ethanol for 48 h, dried in an oven, pressed uni-axially into a disc (diameter: 24 mm), and pre-sintered at 1250 °C for 3 h to prepare an anode-support. The LDC buffer layer was then coated on to the anode by repeated dipping in a suitably prepared slurry and co-fired at 1400 °C for 4 h. The LSGM electrolyte layer was formed likewise. The thickness of each layer was controlled by adjusting the number of dip-coatings. Finally, double layers of LSM ($La_{0.85}Sr_{0.15}MnO_3$)–LSGM composite and LSCF ($La_{0.6}Sr_{0.4}Co_{0.2}Fe_{0.8}O_3$) were coated as a cathode successively on top of the LSGM layer by screen printing. The single cell was ready for the test after firing the cathode layer at 1200 °C for 3 h. The BSE (back-scattered electron) micrograph in Fig. 1(b) shows a cross-sectional view of the single cell. Dry hydrogen and air were fed as fuel and oxidant gases, respectively. Both gases were supplied at the same flow rate of 100 ml min^{-1} by mass-flow controllers.

3. Results and discussion

3.1. Characterization of LSGMs

The XRD patterns of LSGM8080 and LSGM8083, which have a single phase of perovsikte structure in their as-sintered states, are shown in Fig. 2. According to the XRD patterns that have been presented by Datta et al. [7], LSGM8080 synthesized by a solid-state reaction contains very little of the above-mentioned second phases.

The SEM images of the two LSGMs are given in Fig. 3. The average grain sizes are estimated from the images and summarized in Table 1, together with the relative densities measured using the Archimedes method. No practical differences can be found in the

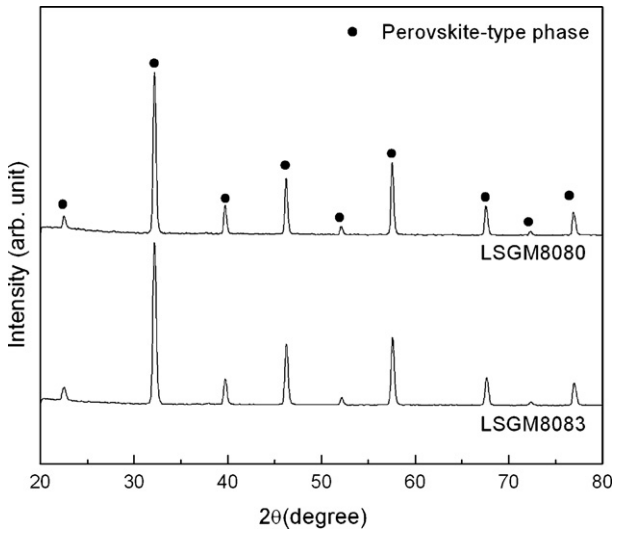

Fig. 2. XRD patterns of LSGM8080 and LSGM8083 sintered at 1400 °C for 4 h.

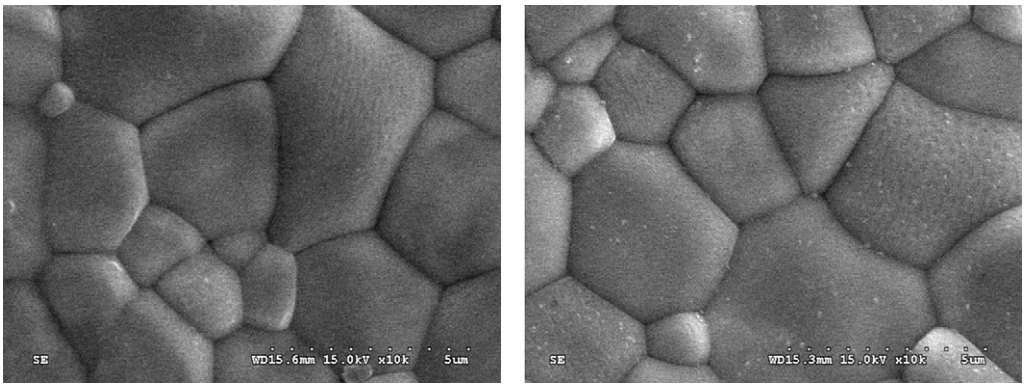

Fig. 3. SEM images of LSGM8080 (left) and LSGM8083 (right) sintered at 1400 °C for 4 h.

Table 1
Average grain sizes and relative densities for LSGM8080 and LSGM8083 sintered at 1400 °C for 4 h.

Composition	Average grain size (μm)	Relative density (%)
LSGM8080	3.9	99.5
LSGM8083	3.7	99.3

two images. Both show well-developed grains with quite similar average sizes. The grains are arranged densely with no visible pores between them and, as can be seen in the Table, the values of the relative density are over 99% for the two LSGMs, meaning that they were both well sintered. Fig. 4 shows the Arrhenius plot for the electrical conductivity of the two LSGMs. According to the data, the electrical conductivity of LSGM8080 is slightly higher than that of LSGM8083 over the whole range of temperature chosen for the measurements. At 800 °C, for example, the electrical conductivity values for LSGM8080 and LSGM8083 are 0.144 and 0.116 S cm^{-1}, respectively. Electrical conductivity tests were performed four or five times and the measurement error was ±5%. The value of 0.144 S cm^{-1} for LSGM8080 is more than three times as high as ~0.045 S cm^{-1} reported for YSZ at 800 °C [8] and even higher than ~0.1 S cm^{-1} for YSZ at 1000 °C. Thus, it can be said that LSGM8080 is a promising electrolyte for IT-SOFCs.

The above finding, however, is contrary to that of Huang et al. [6] for which LSGM8083 showed higher electrical conductivity than LSGM8080 in the temperature range of 600 to 800 °C. This may have been caused by the different synthesis methods used for the LSGM powders or by their different grain structures.

3.2. Chemical stability of LDC buffer layer material

An Ni–YSZ cermet is generally used as the anode in the case of an YSZ electrolyte. Likewise, an Ni–LSGM cermet would be the natural choice as the anode material in the case of an LSGM electrolyte. It was observed in our laboratory, however, that LSGM8080 reacted extensively with Ni to form an insulating product phase of $LaNiO_3$ [6], as mentioned above. It was therefore concluded that LSGM would not be an adequate skeleton material for the anode. Furthermore, the anode containing Ni should not be in direct contact with the LSGM electrolyte. A chemically-stable buffer layer has to be inserted between the anode and electrolyte layers. Some searches were made for a proper material and, after a few trials, LDC was finally chosen.

Figs. 5 and 6 give the XRD patterns of the LDC/NiO and LDC/LSGM8080 mixtures, respectively, before and after heating at 1400 °C for 4 h. In both figures, the XRD patterns before and after heating are practically the same and no extra peaks for reaction product phases can be seen. This means that the LDC is inert to both NiO and LSGM8080 and therefore can be used as a material for the buffer layer, as well as for the skeleton of the anode.

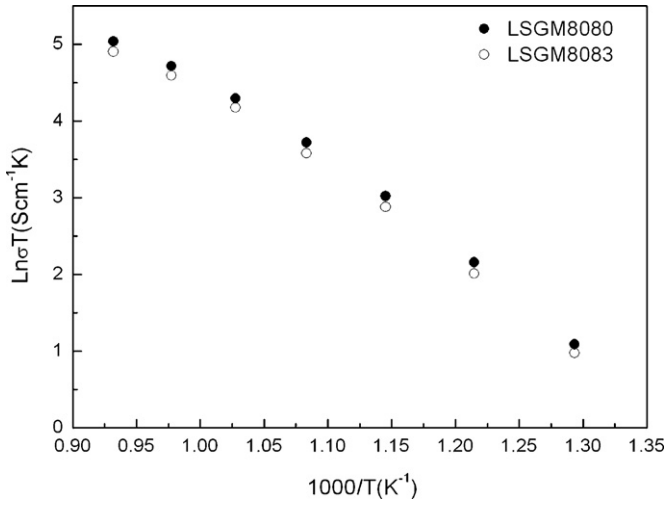

Fig. 4. Arrhenius plot for ionic conductivity of LSGM8080 and LSGM8083 sintered at 1400 °C.

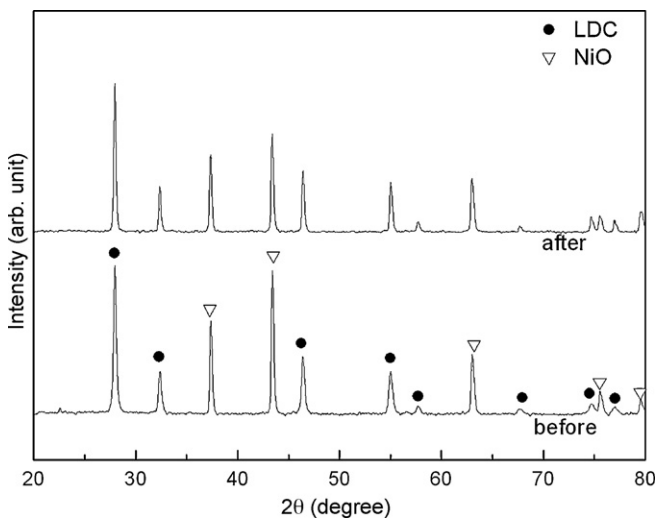

Fig. 5. XRD patterns of LDC/NiO mixture before and after heating at 1400 °C for 4 h.

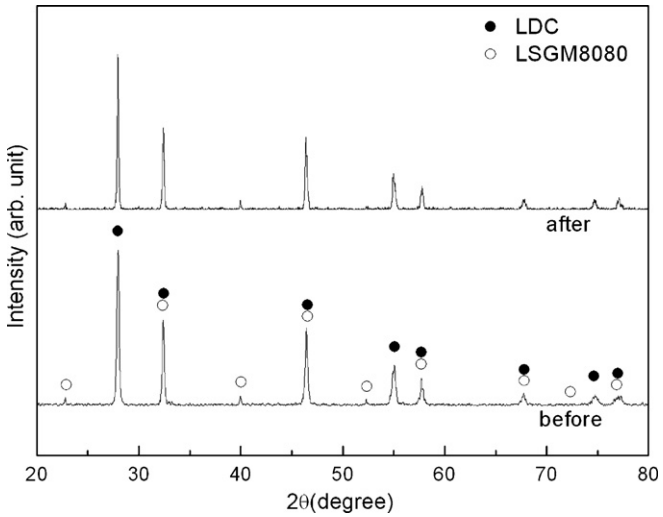

Fig. 6. XRD patterns of LDC/LSGM8080 mixture before and after heating at 1400 °C for 4 h.

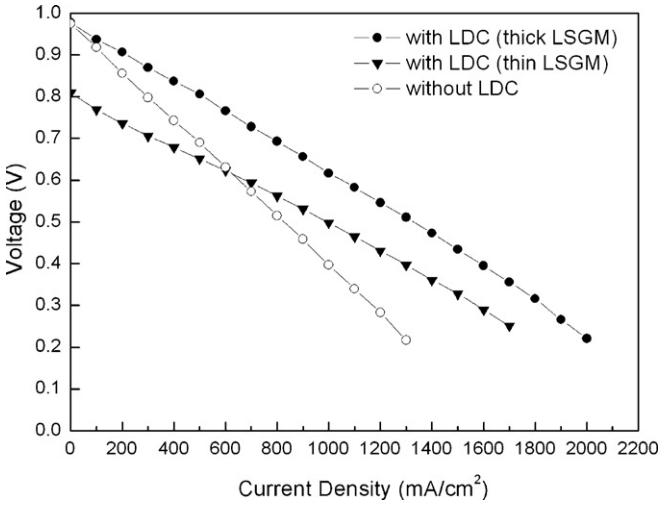

Fig. 8. Comparison of cell performances in cases with and without an LDC buffer layer at 800 °C.

As a final verification before its use, the electrical conductivity of LDC was measured. It turned out to be about the same as that of YSZ.

3.3. Single-cell performance

The current density–voltage (*I–V*) and current density–power density (*I–P*) characteristics of a cell with a (NiO + LDC)|LDC|LSGM|cathode configuration at 750 and 800 °C are shown in Fig. 7. In order to minimize the ohmic losses, the LDC buffer layer and the LSGM electrolyte layer were made as thin as 15 and 20 μm, respectively. The value of the open-circuit voltage (OCV) normally expected from the theoretical calculation (high heating value basis) for a typical solid oxide fuel cell operating at 800 °C is 0.978 V [9]. However, as can be seen in the Fig. 7, the OCV is 0.81 V at 800 °C, which is lower than the expected value, and 0.84 V at 750 °C. The maximum power density is 517 and 426 mW cm^{-2}, respectively.

Efforts were made to find the possible causes for the low OCV observed in Fig. 7. First of all, the reproducibility of the experimental data was checked by repeating the same single-cell test. Then, for comparison, another single-cell test was performed using the same cell but without an LDC layer. Fig. 8 compares the polarization curves for the cells with and without an LDC layer at 800 °C. It can be easily seen that the cell without an LDC layer shows a higher OCV (0.98 V) than that with an LDC layer. The OCV of 0.98 V for the former is quite close to the theoretically expected value. The cell without an LDC layer also shows a lager IR drop (the slope of the *I–V* curve) than that with an LDC layer. This large IR drop must have been caused by the product phase ($LaNiO_3$) resulting from the aforementioned chemical reaction between Ni and LSGM.

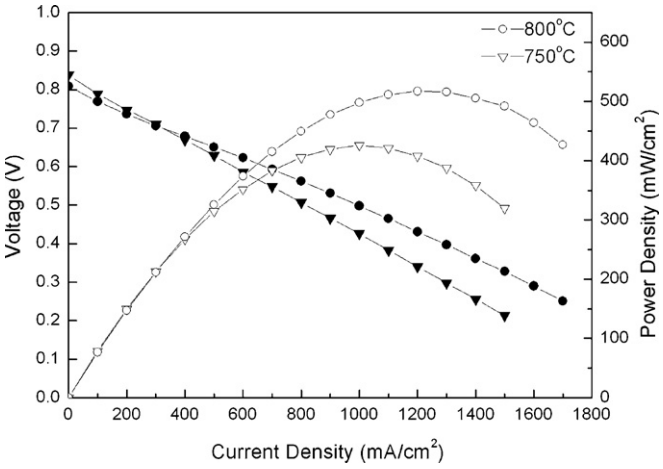

Fig. 7. Performance of single-cell (thin LSGM) with LDC buffer layer at 750 and 800 °C.

The only difference between the two cells is the presence or absence of an LDC buffer layer. Therefore, it is natural to assume that the low OCV originates from the LDC layer. It is well known that, in the case of ceria-based electrolyte such as LDC, some Ce^{4+} ions are reduced to Ce^{3+} in a reducing atmosphere and rise to increased electron conduction and thus internal currents. According to the theory on fuel cell irreversibilities, the internal current is supposed to shift the polarization curve to the lower current side by the amount of the internal current and thus causes a voltage drop at open-circuit [9]. Besides, the LSGM layer is too thin to block the electron flow from the LDC layer. Recently, Bi et al. [10] encountered the same situation as found here when conducting performance tests of an anode-supported solid oxide fuel cell with a bilayered LDC/LSGM electrolyte. They investigated systematically the effect of LSGM layer thickness on the OCV and concluded that electron flow from the LDC layer cannot be blocked completely by an LSGM layer with a thickness of less than 50 μm [10].

On the basis of the conclusion of Bi et al. [10], an attempt was made to thicken gradually the LSGM layer by increasing the number of dip-coatings. Finally, as can be seen in Fig. 8, the OCV of the cell at 800 °C increased from 0.81 to 0.98 V, which is the same as the value for the cell without an LDC layer, when the LSGM layer was thickened from 20 μm (thin LSGM) to 60 μm (thick LSGM) with the other conditions kept the same as those corresponding to Fig. 7. The 60 μm thick LSGM layer thus seems to be thick enough to block electron flow from the LDC layer. The IR drop for the cell with the thick LSGM is a slightly larger than that for the cell with the thin LSGM, but not as large as would be expected given that the LSGM layer has been triply thickened. Fig. 9 shows the *I–V* and *I–P* characteristics at 750 and 800 °C for the cell with the thick LSGM layer. The OCV obtained from the experimental data is 0.99 V at 750 °C and the maximum power densities at 800 and 750 °C are 664 and 459 mW cm^{-2}, respectively. At 800 °C, for example, a ~28% increase in the maximum power density has thus been achieved simply by thickening the LSGM layer.

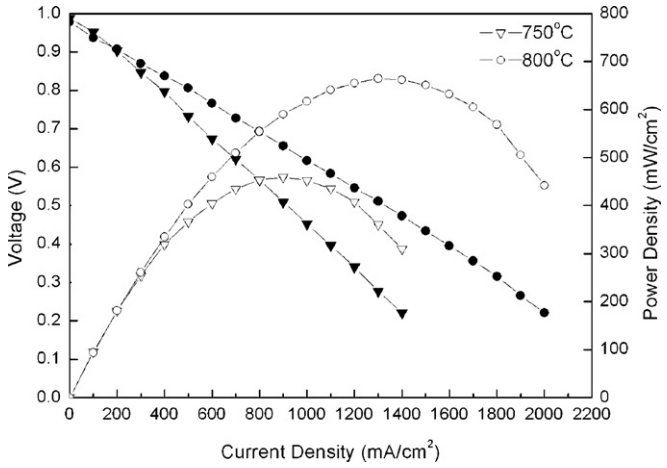

Fig. 9. Performance of single cell (thick LSGM) with LDC buffer layer at 750 and 800 °C.

4. Conclusions

The performance of LSGM ($La_{1-x}Sr_xGa_{1-y}Mg_yO_{3-\delta}$) as the electrolyte for IT-SOFCs has been evaluated using an anode-supported single-cell at intermediate-temperatures of 750 and 800 °C. A chemically-stable LDC (45 mol% lanthanum-doped ceria) buffer layer is inserted between the layers of the Ni–LDC cermet anode and LSGM electrolyte to prevent reaction between Ni and LSGM at the anode|electrolyte interface. The composition of LSGM chosen is the one with both *x* and *y* equal to 0.2, which is proven to have the highest conductivity when prepared by the glycine nitrate process.

The cell shows relatively poor performance with a lower OCV (0.81 V at 800 °C and 0.84 V at 750 °C) than the theoretically calculated value when the LSGM layer is thin (20 μm). On the other hand, when the LSGM layer is thickened to 60 μm, which is thick enough to block electron flow from the LDC buffer layer, an OCV very close to the theoretical value is obtained (0.98 V at 800 °C and 0.99 V at 750 °C). The maximum power densities are 664 and 459 mW cm^{-2} at 800 and 750 °C, respectively.

Acknowledgement

This study was financially supported by the Korea Institute of Energy Research.

References

[1] K.Q. Huang, M. Feng, J.B. Goodenough, J. Am. Ceram. Soc. 79 (1996) 1100.
[2] T. Ishihara, H. Matsuda, Y. Takita, J. Am. Chem. Soc. 116 (1994) 3801.
[3] M. Feng, J.B. Goodenough, Eur. J. Solid State Inorg. Chem. 31 (1994) 663.
[4] K. Huang, R.S. Tichy, J.B. Goodenough, J. Am. Ceram. Soc. 81 (2 (3)) (1998) 2565.
[5] K. Huang, R. Tichy, J.B. Goodenough, J. Am. Ceram. Soc. 81 (1998) 2581.
[6] D. Lee, J. Han, Y. Chun, R. Song, D.R. Shin, J. Power Sources 166 (2007) 35.
[7] P. Datta, P. Majewski, F. Aldinger, J. Alloys Compd. 438 (2007) 232.
[8] Y. Arachi, H. Sakai, O. Yamamoto, Y. Takeda, N. Imanishi, Solid State Ionics 121 (1999) 133.
[9] J. Larminie, A. Dicks, Fuel Cell Systems Explained, 2nd ed., Wiley, 2003.
[10] Z. Bi, Y. Dong, M. Cheng, B. Yi, J. Power Sources 161 (2006) 34.